ELSEVIER

Catalysis Today 59 (2000) 19–31

CATALYSIS TODAY

www.elsevier.com/locate/cattod

Methane combustion on perovskites-based structured catalysts

S. Cimino[a,*], L. Lisi[b], R. Pirone[b], G. Russo[b], M. Turco[a]

[a] *Dipartimento di Ingegneria Chimica, Università degli Studi di Napoli "Federico II", P.le Tecchio 80, 80125 Napoli, Italy*

[b] *Istituto Ricerche sulla Combustione — CNR, P.le Tecchio 80, 80125 Napoli, Italy*

Abstract

$LaMnO_3$ perovskites supported on La stabilised γ-Al_2O_3 and MgO have been prepared and characterised as methane combustion catalysts. XRD analysis, BET surface area results and H_2 TPR measurements have all revealed the presence of significant interaction between the perovskite and the alumina based support, which becomes very strong upon thermal treatment at 1100°C. On the other hand, MgO supported samples undergo only sintering processes with reduction of surface area upon treatment at 1100°C. Catalytic activity measurements in methane combustion have been performed both in fixed bed and in monolithic reactor. The results on powders have shown that the dispersion on both supports is effective to enhance the catalytic performances of the catalysts treated at 800°C. A very strong deactivation is observed for the La/Al_2O_3 supported catalyst when pre-treated at 1100°C, while $LaMnO_3$/MgO shows a promising high thermal stability. The chemical nature of the active sites changes by dispersing $LaMnO_3$ on both supports, even if to a different extent, as revealed by the estimated values of apparent activation energy and reaction orders for methane and oxygen.

Structured combustion catalysts have been prepared following well established procedures to washcoat commercial cordierite monoliths with lanthanum stabilised alumina. The subsequent deposition of precursors on the coated monolith has been obtained by deposition precipitation method. Comparison between monolith and corresponding powder sample shows a higher catalytic activity of the former, likely to be attributed to the better dispersion obtained with repeated deposition cycles of active phase on the thin washcoat layer. Moreover, a lower deactivation has been observed on monolith after ageing under reaction at 1050°C for 2 h, suggesting promising developments of this technique to produce catalytic combustion systems for high temperature applications.

Keywords: Methane combustion; Perovskites; Supported catalysts; Monoliths

1. Introduction

Catalytic combustion is an attractive way to produce thermal energy of high quality from the environmental point of view, since it allows efficient and complete fuel burning at temperatures lower than in the flame combustion and without yielding undesired by-products, such as UHC, CO, NO_x and particulate [1,2]. One of the most interesting potential applications of the catalytic combustion is in the natural gas fuelled burners for gas turbine power generation [3]. The very high temperatures in this process demands to the researchers very hard tasks, since an unavoidable contrast between activity and stability has to be taken into account in the choice of the material. PdO is active already at low temperature but cannot stand temperatures higher than 800°C [4] and must be therefore protected from overheating. Its use in high temperature applications should be restricted to the ignition section of the reactor, the complete combustion being homogeneously achieved in the gas phase or in more stable catalytic segments in the final section of the burner [5,6]. On the other hand, hexaaluminates are very stable at elevated temperatures but their

* Corresponding author.

0920-5861/00/$ – see front matter
PII: S0920-5861(00)00269-8

activity is very low, making them interesting only in the last stages of a multimonolith configuration [6].

In recent years, a lot of research effort has been devoted to the study of perovskite-type oxides in catalytic combustion [7]. These materials have a general ABO_3 structure and show quite promising activity even at moderate temperatures and good heat resistance up to about 2000°C [7,8]. The number of perovskites with potential interest in the oxidation reactions is very great, owing to the number of A and B cations being able to enter in this structure and the possibility to partially substitute either A and/or B position (general formula $A_xA'_{1-x}B_yB'_{1-y}O_3$). Up to now, the best catalytic performances in fossil fuel combustion are exhibited by La or La–Sr based perovskites (in A position) containing Co, Fe or Mn as B cation [8,9].

Nevertheless, the application of perovskite is still limited by their low surface area and strong tendency to sinter. Conventional preparation methods need both long time and high temperatures in order to achieve the ABO_3 structure, resulting in very low surface area. Recent studies on the preparation methods of perovskites have been focused to the production of higher surface area catalysts. Despite some very interesting results achieved with preparation at lower temperatures (in particular by means of citrates precursors, sol–gel and freeze-drying methods), the surface area of these catalysts decreases very strongly upon treatment at elevated temperatures (above 900°C). A different approach to increase both surface area and mechanical strength of perovskites is their dispersion on a high surface area support [10–16].

Alumina is the most widely used support but tends to loose its high surface area under severe operating conditions typical of the combustion process. Transition aluminas start to loose area even below 800°C due to elimination of micropores, but the critical loss occurs above 1000°C with the transition to thermodynamically stable α-phase [17]. As reviewed by Arai and Machida [18], kinetic inhibition of sintering processes can be achieved by several additives, La_2O_3 being the most effective. One of the first attempts in preparing perovskite supported catalysts for methane combustion was made by Zhang et al. [10]. They succeeded in supporting $La_{0.8}Sr_{0.2}MnO_{3+x}$ perovskite prepared by citrates method on $La_2O_3{\bullet}19Al_2O_3$ or Mn_2O_3 modified $La_2O_3{\bullet}19Al_2O_3$. It must be noticed that thermal treatment at elevated temperature causes a marked reduction of activity due to the loss of surface area of the support. Moreover results obtained with $LaCrO_3/Al_2O_3$ in methane combustion after ageing at 1340 K [11] showed that the deactivation is even higher than what is expected only by the surface area decrease. Chemical interaction between support and active phase must be implied, as shown in [12], where the authors reported the formation of a mixed perovskite phase $LaCr_xAl_{1-x}O_3$ at 1100°C for the $LaCrO_3/Al_2O_3$ system and at 1200°C for $LaCrO_3/LaAl_{11}O_{18}$. Arnone et al. [16] evidenced a measurable interaction between the active phase and the support after a 3 h treatment at 1100°C in flowing air of $LaMnO_3$ supported on La_2O_3/Al_2O_3.

High thermal stability has been reported by Marti et al. [13] for aluminate spinels MAl_2O_4 (M=Mg, Ni and Co), used as supports for $La_{0.8}Sr_{0.2}MnO_{3+x}$ active phase. In those support materials the alumina lattice was saturated with bivalent metal ions so that no further migration of Mn from the active phase is possible.

Magnesia has also been proposed as support for combustion catalysts for its thermal stability exceeding that of alumina [18–21]. Moreover, no negative interaction of perovskite with the support has been found by Saracco et al. [15], with a series of $LaCr_xMg_{1-x}O_3$ perovskites dispersed on MgO.

In some applications of catalytic combustion, such as in gas turbine combustors, structured catalysts must be used since they allow to minimise pressure drops [22]. Monolithic reactors have been intensively studied in recent years for either $DeNO_x$ [23] and catalytic combustion processes [22,24,25], but very few examples of perovskite-based structured catalysts have been reported for catalytic combustion. Ciambelli et al. [14] have investigated the catalytic performances of a series of extruded monoliths made of perovskite powders (La–Ce or Dy–Y in A position and Ni, Fe and Mn in B position). The comparison with the corresponding powder catalysts showed similar values of apparent activation energy for methane combustion, although with a not complete selectivity to CO_2. More conventional procedures are based on covering cordierite monoliths with perovskite containing active phase. Arai and Machida [18] reported that honeycomb coating with perovskite–water slurry resulted in lower stability with respect to mono-

liths made of manganese-substituted hexaaluminates $Ba_{0.8}K_{0.2}MnAl_{11}O_{19}$. Zwinkels et al. [12] supported $LaCrO_3$ on a γ-Al_2O_3 washcoated cordierite monolith. The supported catalyst was characterised as powder, while the activity data were obtained only with the monolithic reactors, so no comparison could be drawn between the characteristics of monolith and the precursor $LaCrO_3/Al_2O_3$ and $LaCrO_3/LaAl_{11}O_{18}$ powder particles. However it is evident, following this second more classical approach to obtain perovskite-based monoliths, that the study of the dispersion of the active phase on a washcoat support is very necessary.

In this work we have investigated the catalytic properties in methane combustion of $LaMnO_3$ perovskites, supported on La stabilised γ-Al_2O_3 and MgO, in order to combine high activity at low temperature, related to the higher surface area, with wider range of thermal stability due to the dispersion on the supports. Catalytic systems have been prepared as powders in order to characterise their physico-chemical properties and assess the influence of support on the catalytic features in methane combustion. Moreover, catalysts have also been prepared in the form of monoliths to compare the catalytic properties with those of powder samples in terms of ignition behaviour, catalytic performances and thermal stability.

2. Experimental

2.1. Catalyst preparation

2.1.1. Alumina supported $LaMnO_3$

Commercial γ-Al_2O_3 (CK 300 with 200 m^2/g, Akzo Chemie) was stabilised with 5 wt.% La_2O_3 using the wet impregnation technique. The alumina powder was suspended in an aqueous solution of $La(NO_3)_3{\bullet}6H_2O$ (Fluka, >99%) and the excess water removed in a rotary evaporator at 55°C under reduced pressure. After drying at 120°C, the powder was calcined in flowing air (100 N cm^3/min) at 800°C for 3 h, in order to decompose the nitrate.

$LaMnO_3$ was deposited on the stabilised alumina from nitrate and acetate precursors with the deposition precipitation (DP) method, previously reported for the preparation of metal oxides supported catalysts [26]. Stabilised γ-Al_2O_3 powder was suspended in a solution of suitable amounts of lanthanum nitrate, manganese acetate ($C_4H_6MnO_4{\bullet}4H_2O$, Sigma, >99%) and urea (CH_4N_2O, Fluka, >99.5%) (molar ratio urea/cationic species 9:1) heated to 90°C for 5 h under stirring. At this temperature urea slowly decomposes producing ammonia homogeneously in the suspension, thus causing the preferential co-precipitation of hydroxides inside the pores of the support. The $LaMnO_3$ nominal loading in the catalysts was 30 wt.%. After removing the excess water and drying at 120°C, the powder was treated in flowing air at 800°C for 3 h. Part of this catalyst was further treated at 1100°C for 3 h.

2.1.2. Bulk $LaMnO_3$

A bulk perovskite sample was also prepared by co-precipitation, using urea as a base, as for the DP method. A solution of lanthanum nitrate, manganese acetate and urea (molar ratio urea/cationic species 9:1) was heated to 90°C for 5 h under continuous stirring. After removing the excess water, the resulting powder was dried at 120°C and calcined in flowing air at 800°C for 3 h.

2.1.3. MgO-dispersed $LaMnO_3$

Magnesium oxide was obtained by thermal decomposition of carbonate ($(MgCO_3)_4{\bullet}Mg(OH)_2{\bullet}5H_2O$, Carlo Erba, >99%) at 800°C for 3 h. Suitable amounts of lanthanum nitrate and manganese acetate to obtain 20 wt.% loading of perovskite in the catalyst were dissolved in water and MgO powder added under stirring. Due to its basic nature, MgO partially dissolved and the pH increased to a constant value of 10.5, causing the precipitation of metal hydroxides. The excess water was removed in the rotary evaporator at 55°C under reduced pressure. After drying at 120°C, the powder was calcined in flowing air (100 N cm^3/min) at 800 or 1100°C for 3 h.

Table 1 reports the nominal compositions and calcination temperatures of powder catalysts.

2.1.4. Monolith catalysts

Cordierite monoliths (Corning) with a cell density of 400 cpsi were cut to obtain samples with 25 channels cross-section. Monoliths were washcoated with alumina by dipping samples in a slurry of finely grounded γ-Al_2O_3 powder, diluted nitric acid solution

Table 1
Nominal compositions and identification code of catalysts

Catalyst ID	Nominal composition	Calcination temperature (°C)
LaMn	$LaMnO_3$	800
Al	5% La_2O_3/Al_2O_3	800
Mg	MgO	800
3-Al-8	30% $LaMnO_3$/(5% La_2O_3/Al_2O_3)	800
2-Mg-8	20% $LaMnO_3$/MgO	800
3-Al-11	30% $LaMnO_3$/(5% La_2O_3/Al_2O_3)	1100
2-Mg-11	20% $LaMnO_3$/MgO	1100

and pseudobohemite (Disperal, Condea Chemie) [27]. The total amount of solids in the slurry was 20 wt.%. Several dips were needed to obtain the desired amount of washcoat loading (approximately 25% of the total weight). In each cycle the excess slurry was removed by blowing air through the channels, after which the samples were dried at 120°C and then calcined at 550°C for 3 h. La_2O_3 (5 wt.%) was added to the alumina washcoat by impregnation in a water solution of lanthanum nitrate, followed by drying at 120°C and calcination at 800°C for 3 h. The $LaMnO_3$ active phase was added to the monolith samples using the DP method already employed for the preparation of the powder catalyst. In this case the monolith sample was suspended in the solution continually stirred. Several cycles were needed to reach the target loading of 30 wt.% of perovskite. After each cycle, the monolithic samples were calcined at 800°C for 3 h.

2.1.5. Physico-chemical characterisation

X-ray diffraction (XRD) analysis was performed using a Philips PW 1710 diffractometer. Specific surface area of the catalysts was evaluated by N_2 adsorption at 77 K according to the BET method using a Carlo Erba 1900 Sorptomatic apparatus.

Temperature-programmed reduction (TPR) experiments were carried out with Micromeritics 2900 apparatus equipped with a thermal conductivity detector (TCD). After a treatment in airflow at 800°C, the sample was reduced with 5% H_2/Ar mixture (30 cm^3/min) heating 10°C/min up to 800°C.

2.1.6. Experimental apparatus for catalyst testing

Catalytic combustion experiments were carried out with a quartz down flow reactor electrically heated in a three zones tube furnace. The reactor had an annular cross-section in the case of powders in order to obtain a small equivalent diameter that enables to control catalyst temperature and to reduce the temperature gradients within the bed. Catalyst particles in the range of 180–250 μm were diluted with quartz powders of the same dimension to approach reactor isothermicity and placed on a porous quartz disk. The temperature of the catalytic bed was measured by a K-type thermocouple placed inside the inner quartz tube, and axial gradients were verified to be always $\leq$3°C. For monolithic catalysts the external and central channels were blocked at both ends with ceramic wool, leaving eight free channels on the cross-section. The central channel was used to measure the monolith temperature with a sliding thermocouple. The narrowing of the reactor section in pre- and post-catalytic zone and the presence of quartz pellets upside the catalytic bed limited the occurrence of homogeneous reactions. The gaseous flow rates were measured by Brooks 5850 mass flow controllers and mixed at atmospheric pressure to obtain variable inlet concentrations of reactants. The feed and product streams were analysed by on line HP 6890 gas cromatograph with thermal conductivity and flame ionisation detectors, equipped with Porapak Q and molecular sieve 5A columns. All catalysts were tested twice and for each test the methane conversion was calculated as the average of at least three measurements. Carbon balance was close to within ±5% in all catalytic tests.

3. Results

3.1. XRD results

Table 2 reports the XRD phases and the surface area of the catalysts and the supports investigated. The

Table 2
Surface areas and XRD phases of powder catalysts and supports treated at different temperatures in flowing air (Minorphases in parenthesis)[a]

Catalyst	Calcination temperature (°C)			
	800		1100	
	XRD phases	BET (m^2/g)	XRD phases	BET (m^2/g)
LaMn	P, (LO)	11	–	–
Al	γ	178	γ, (θ)	118
3-Al-8	γ	88	–	–
3-Al-11	–	–	P, PA, LA, LO, MO	4
2-Mg-8	P, MgO	25	–	–
2-Mg-11	–	–	P, MgO	5

[a] Legend: γ, θ: γ, θ alumina phases; P: $LaMnO_3$ perovskite; PA: $LaAlO_3$ perovskite; LA: aluminium–lanthanum oxides; LO: lanthanum oxide; MO: manganese oxides; MgO: magnesium oxide.

results show that a calcination temperature of 800°C is not sufficient to obtain a pure unsupported $LaMnO_3$ perovskite phase, as shown by the presence of traces of La_2O_3 and $La(OH)_3$ in the LaMn sample. The γ-Al_2O_3 used as support has a poor crystallinity and the treatment at 800°C of the La_2O_3 stabilised sample does not cause any increase of crystal size. On the other hand, treating the stabilised support at 1100°C results in the partial transition from γ to θ phase characterised by a lower surface area. The transition to α phase of alumina at 1100°C is inhibited by the presence of La_2O_3 due to the formation of surface lanthanum aluminate [17,18]. The deposition of $LaMnO_3$ on alumina does not promote any phase transition of the support upon calcination at 800°C. Furthermore, no signals of the perovskite phase have been detected, likely due to the high dispersion of the active phase. On the contrary, calcination at 1100°C results in the formation of perovskite crystals, as also observed by Zwinkels et al. [12] for $LaCrO_3$ supported perovskite. Moreover, in this case the presence of the active phase enhances the reaction between lanthanum and aluminium oxides leading to the formation of $LaAlO_3$ and other aluminium–lanthanum mixed oxides. Some signals of lanthanum and manganese oxides have also been detected for this sample. Finally, a dramatic reduction of the surface area of the 3-Al-11 sample is observed, stronger than that found after calcination at 1100°C on the Al sample which does not contain any active phase.

The dispersion of $LaMnO_3$ on MgO does not result in any interaction inhibiting the formation of the target perovskite phase compounds either after calcination at 800°C or at 1100°C, as reported by Saracco et al. [15] for the system $LaCrO_3$–MgO. However, thermal treatment at 1100°C gives rise to a significant reduction of the surface area due to the increase of the crystal size, as also confirmed by sharper peaks observed in the XRD spectrum of the 2-Mg-11 sample.

3.2. Temperature programmed reduction

TPR profiles of the supported catalysts are showed in Fig. 1 compared with unsupported $LaMnO_3$ perovskite. The H_2 consumption and the temperature corresponding to the maximum H_2 uptake are reported in Table 3. Since at least two main signals can be identified in all TPR profiles, the total H_2 consumption has been divided into two contributions at low (first step) and high temperature (second step), respectively.

As previously reported [28] the reduction of bulk $LaMnO_3$ perovskite leads to the formation of MnO and La_2O_3 due to the simultaneous reduction of manganese to Mn^{2+} and loss of the perovskite structure. The value of the H_2/Mn ratio corresponding to the total H_2 consumption higher than the stoichiometric one for the reduction of Mn^{3+} to Mn^{2+}, indicates for LaMn sample the presence of a fraction of Mn^{4+} (15% of total) in the perovskite structure. The reduction process occurs in two main steps as clearly shown by the two peaks of the TPR profile, the first one with maximum at about 435°C and the second one approaching the isothermal region. They were attributed to the reduction of Mn^{4+} to Mn^{3+} and of Mn^{3+} to Mn^{2+}, respectively [28].

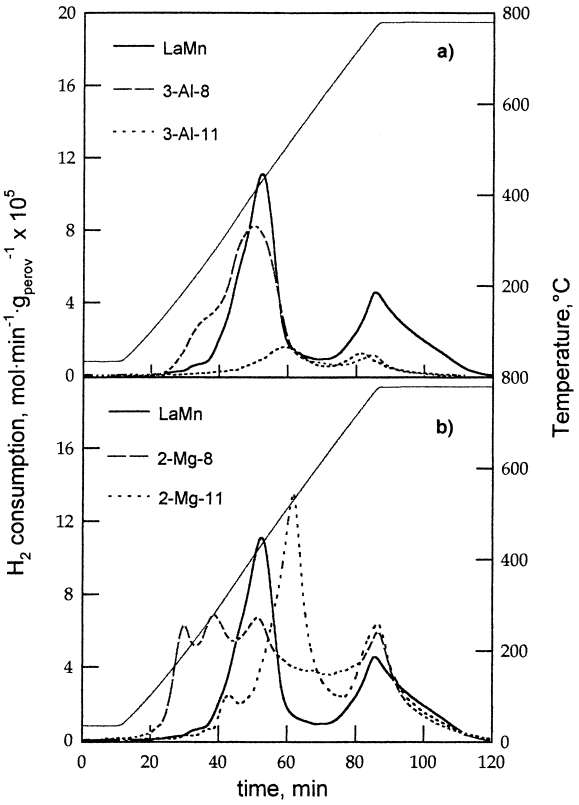

Fig. 1. TPR profiles of supported catalysts as compared with unsupported $LaMnO_3$. (a) Alumina supported samples; (b) magnesia dispersed samples.

The supported samples show some peculiar differences with respect to the bulk perovskite that can be attributed to the interaction with support itself, since neither stabilised alumina nor MgO undergo any reduction under experimental conditions investigated. Regarding the catalysts supported on lanthanum stabilised alumina, 3-Al-8 sample gives a total H_2/Mn ratio slightly lower than 0.5, indicating an apparent average oxidation state of manganese lower than 3. This result suggests that a fraction of Mn is not available for the reduction due to both physical and chemical incorporation into the alumina lattice even upon a not severe thermal treatment (800°C). However, the different features of the TPR can also be attributed to the presence of some Mn_2O_3 and Mn_3O_4 in the catalyst. This circumstance could be confirmed by the lower activation energy, typical of simple oxides [16], evaluated for 3-Al-8 sample and for the monolith, if compared with that of the bulk perovskite treated at the same temperature. Treatment of 3-Al-11 sample at 1100°C results in a dramatic decrease in the H_2 consumption. Such a low value corresponds to a large reduction of intensity of both peaks and is due to the stronger interaction of manganese with alumina, promoted by the higher calcination temperature, revealed by the XRD analysis showing the formation of new crystalline phases.

The TPR curves of MgO supported perovskites catalysts show some peculiar features. The amount of H_2 consumed for the 2-Mg-8 catalyst is extremely high and indicates an average initial oxidation state of manganese of 3.7. Moreover, the onset temperature of reduction is 150°C lower (starting at 100°C) than for bulk LaMn sample and the signal in the first zone shows a very complex shape resulting from the partial overlapping of three peaks of comparable intensity. On the contrary, the peak in the second reduction step is similar to that found in the TPR profile of the bulk LaMn perovskite. Since no other phases except MgO and perovskite were found by XRD analysis, the high reducibility of this sample could be related to the formation of a Mg partially substituted nonstoichiometric perovskite, in which a large part of Mn is

Table 3
H_2 consumption measured in TPR of catalysts

Catalyst	Total H_2 consumption (mol H_2/mol Mn)	First step		Second step	
		H_2 consumption (mol H_2/mol Mn)	T_{max} (°C)	H_2 consumption (mol H_2/mol Mn)	T_{max} (°C)
LaMn	0.565	0.345	434	0.220	≥790
3-Al-8	0.470	0.420	410	0.050	≥790
3-Al-11	0.085	0.050	506	0.035	≥790
2-Mg-8	0.850	0.540	430	0.310	≥790
2-Mg-11	0.690	0.430	535	0.260	≥790

forced in the oxidation state 4+ to balance the total charge. Thermal treatment at 1100°C, however, causes a reduction of the total H_2 consumption for 2-Mg-11 sample corresponding to a manganese average initial oxidation state of 3.4, still higher than that found for the unsupported $LaMnO_3$. The shape of the signal is more similar to that of the bulk LaMn sample, giving the same onset temperature and a first reduction step with the presence of a single peak even if with a small shoulder. Therefore, it can be hypothesised that the higher calcination temperature reduces the extent of Mg^{2+} substitution in the perovskite structure, promoting the formation of a better crystallised $LaMnO_3$ perovskite, as confirmed by the sharper XRD peaks shown by 2-Mg-11 sample. As a consequence, the fraction of Mn^{4+} decreases proportionally giving rise to a lower H_2 consumption.

3.3. Catalytic activity measurements

The catalytic activity in methane combustion was measured both on supported catalysts and on MgO and La-stabilised γ-Al_2O_3 supports. Homogeneous reaction tests have also been carried out with the reactor filled with quartz powders in order to evaluate the onset temperature of gas phase reactions. In all experimental conditions investigated, the only reaction product detected on perovskite based catalysts was CO_2, while with both supports and quartz a significant amount of CO was found in the products.

Fig. 2 shows the results of the activity tests carried out in order to compare the catalytic performances in methane oxidation of the powder catalysts prepared. In particular, measured values of methane conversion are reported as functions of the reaction temperature in Fig. 2(a) and (c), and corresponding Arrhenius plots are shown in Fig. 2(b) and (d). Experimental conditions in these measurements were chosen so as to justify the assumption of isothermal catalytic bed. Inlet methane and oxygen concentrations were respectively 0.4 and 10 vol.% (the remaining gas being nitrogen); the contact time, defined as the ratio between the mass of catalyst loaded and the flow rate of the inlet gas mixture (W/F), was 0.09 g·s/N cm^3.

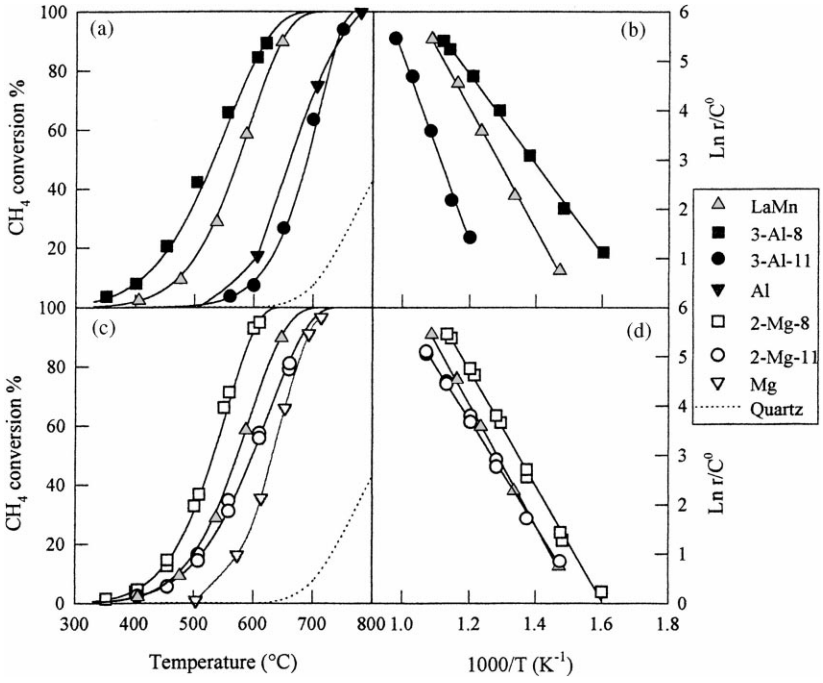

Fig. 2. Effect of temperature on methane combustion for powder catalysts and corresponding Arrhenius plots (0.4% CH_4, 10% O_2, W/F=0.09 g·s/N cm^3). Continuous lines represent fittings with parameters obtained from kinetic analysis.

Table 4
Catalytic performances in methane combustion of $LaMnO_3$ based catalysts

Catalyst ID	T_{10} (°C)	T_{50} (°C)	T_{90} (°C)	E_{act} (kcal/mol)	Reaction rate (500°C) (mmol/g h)	Surface reaction rate (500°C) (mmol/m^2 h)
LaMn	472	575	646	24.4	1.18	0.107
3-Al-8	413	532	622	18.2	2.75	0.031
2-Mg-8	440	533	598	23.3	2.32	0.093
3-Al-11	607	690	740	37.4	0.04	0.010
2-Mg-11	482	599	681	21.6	0.94	0.188
Monolith (46 000 h^{-1})	419	541	633	18.2	7.26	–

The conversion plot obtained with only quartz loaded in the reactor allows us to assume the contribution of the homogeneous reactions as negligible for all catalysts examined.

Dispersion of $LaMnO_3$ perovskite on both La-stabilised alumina and magnesia is effective to enhance the catalytic performances of the samples treated at 800°C. As clearly shown by conversion plots and values of T_{10}, T_{50} and T_{90} in Table 4, both 3-Al-8 and 2-Mg-8 are more active than the corresponding bulk $LaMnO_3$. An increase in the reaction rate per unit mass (reported in Table 4) by a factor larger than 2 is obtained dispersing the active phase on both Al_2O_3 and MgO. No major differences in the overall activity are observed between these two samples, even if it must be noticed that the MgO supported catalyst has lower loading of active phase and surface area. Very similar surface reaction rates (Table 4) and activation energies have been calculated for LaMn and 2-Mg-8 samples, suggesting that dispersion on MgO does not result in major modifications of chemical nature of active sites. The slight reduction in the values of E_{act} for 2-Mg-8 could be related to a partial substitution of Mn^{3+} with Mg^{2+} in the perovskite structure, which is balanced by a higher fraction of Mn^{4+}, as shown by TPR analysis. On the other hand, lower values of both surface reaction rate and activation energy were measured for 3-Al-8. This reveals a significant influence of the alumina surface towards the formation of active sites, whose chemistry could be partially changed by the interaction with the support. The eventual formation of Mn_2O_3 and Mn_3O_4 micro-clusters should be also taken into account, since it has been reported that the activation energy in methane combustion on those manganese oxides is lower than on $LaMnO_3$ perovskite [16].

Thermal treatment at 1100°C reduces the activity of both γ-Al_2O_3 and MgO supported catalysts, but the extent and the nature of this deactivation appear very different in the two cases. Indeed, 2-Mg-11 is only slightly less active than LaMn calcined at 800°C, while the comparison between the reaction rates per unit mass of 2-Mg-8 and 2-Mg-11 shows that the activity is reduced by a factor of about 2.5, even lower than what is expected from the total loss of surface area (reduced five times by the thermal treatment). As a consequence, surface reaction rate results increased. Moreover, the activation energy estimated on 2-Mg-11 was similar to that obtained on 2-Mg-8 and LaMn catalysts.

On the other hand, 3-Al-11 sample undergoes a very strong deactivation due to the thermal treatment at 1100°C. Temperature for 90% conversion increases by 100°C when compared with that of LaMn and by 120°C with that of the corresponding 3-Al-8. The reduction in reaction rate is surely due to the considerable reduction of surface area to only 4 m^2/g, but also the value of activation energy (37 kcal/mol) is much higher than expected. Moreover XRD signals are very different and a much lower H_2 consumption is observed in TPR measurements. These evidences suggest that the chemistry of the catalyst is changed, as a result of a strong interaction between the active phase and alumina, enhanced by the high temperature pre-treatment. The DP method used to disperse the perovskite active phase does not appear to retard nor inhibit its chemical interaction with the support.

A rough kinetics study has been performed for methane combustion on the five catalysts investigated. Several catalytic activity measurements have been carried out by varying both CH_4 and O_2 concentrations in the feed. Different temperature levels

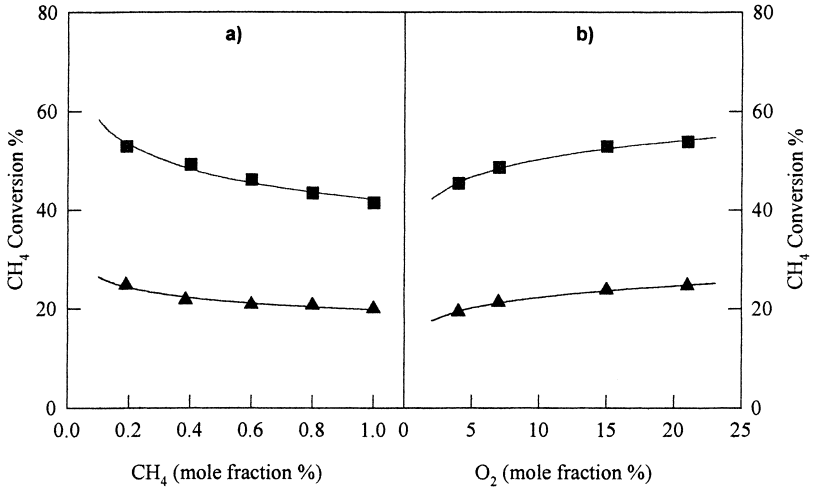

Fig. 3. Methane conversion as a function of the inlet CH_4 (a) and O_2 (b) concentration on LaMn catalyst. T=500°C (▲) or 550°C (■). W/F=0.09 g·s/N cm^3. O_2 inlet concentration 10 vol.% in (a); CH_4 inlet concentration 0.4 vol.% in (b).

have been chosen in order to achieve similar conversions with all the catalysts. Resulting conversion data have been modelled by the power law rate equation: $r = k\, p^n_{CH_4} p^m_{O_2}$, assuming isothermal plug flow conditions. Fig. 3(a) and (b) reports the results obtained on the unsupported LaMn catalyst. A clear reduction of methane conversion to CO_2 is observed by increasing the inlet CH_4 concentration. Since it is possible to assume constant O_2 concentration throughout the reactor in these runs (oxygen being fed in large excess with respect to methane oxidation stoichioimetry), this behaviour is due to a less than linear dependence of the reaction kinetics on CH_4 concentration. The simplified kinetic model used to evaluate methane reaction order on LaMn catalyst: $r = k'\, p^n_{CH_4}$ gives n values weakly variable with temperature and around 0.84 (Table 5). This result is slightly different from the first order dependence reported by Arai et al. [8] for $La_{0.8}Sr_{0.2}MnO_3$ at higher CH_4 partial pressures. Better agreement could be found with the results reported in [8] about the effect of O_2 concentration on CH_4 conversion to CO_2. Fig. 3(b) shows that higher conversions are obtained by increasing oxygen inlet partial pressure over a range of values where it can be still considered to be in large excess. This effect, as modeled by the power law rate equation, reveals a reaction order for O_2 around 0.15, as reported in Table 5.

Table 5
CH_4 and O_2 reaction orders in methane catalytic combustion estimated at several temperatures for all catalysts prepared

Catalyst ID	Temperature (°C)													
	450		500		550		575		600		620		650	
	n	*m*	*n*	*m*	*n*	*m*	*n*	*m*	*n*	*m*	*n*	*m*	*n*	*m*
LaMn			0.86	0.16	0.81	0.14								
2-Mg-8			0.69	0.17	0.72									
3-Al-8	0.77	0.19	0.77	0.19										
2-Mg-11					0.65	0.14	0.70	0.17	0.71	0.18	0.74	0.19		
3-Al-111													0.61	
Monolith		0.18[a]	0.80											

[a] T=420°C.

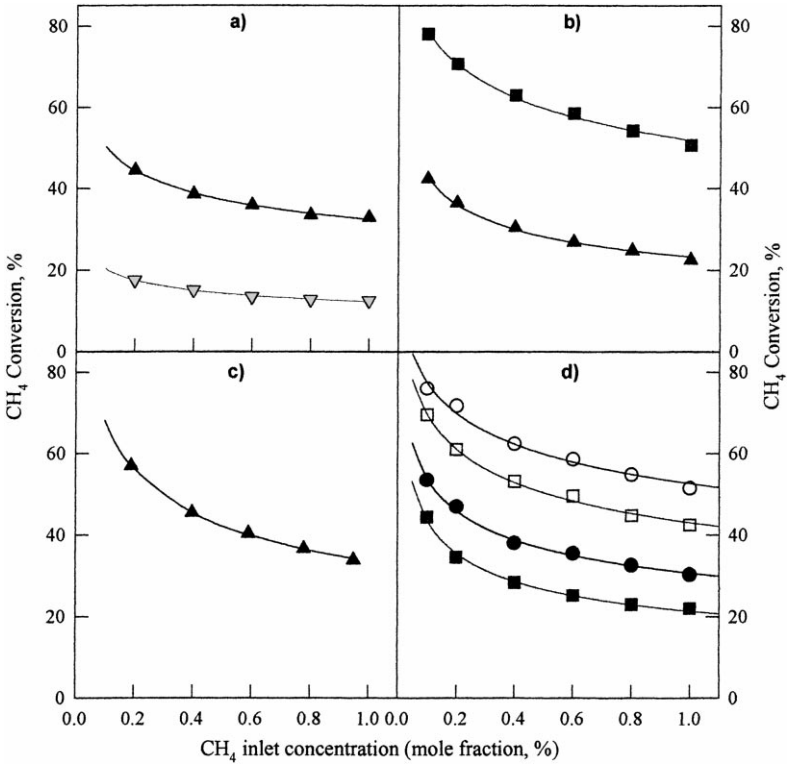

Fig. 4. Methane conversion as a function of the CH_4 inlet concentration over 3-Al-8 (a), 2-Mg-8 (b), 3-Al-11 (c) and 2-Mg-11 (d). Reaction temperature: 450 (▽), 500 (▲), 550 (■), 575 (●), 600 (□), 620°C (○). W/F=0.09 g·s/N cm^3, O_2 inlet concentration=10 vol.%.

The same investigation has been performed on supported perovskite samples too. The results are shown in Figs. 4 and 5, where the effect of inlet CH_4 and O_2 concentrations on methane conversion are presented, respectively.

Also for supported samples a clear decrease in methane conversion to CO_2 occurs by increasing CH_4 inlet concentration, whereas a weak increase is obtained by increasing O_2 inlet concentration. Even if the general behaviour observed is the same, some clear differences should be pointed out.

Table 5 shows that the reaction order of methane over supported catalysts is generally lower than the value found on unsupported LaMn sample (0.81–0.86). This should be related to the interaction with the support which modifies the active sites features. Moreover, on MgO supported catalysts, reaction orders remain quite constant upon treatment at 1100°C, since we estimated n=0.69–0.72 (variable with temperature), m=0.17 on 2-Mg-8 and n=0.65–0.74, m=0.14–0.19 on 2-Mg-11. A different behaviour was revealed by Al supported samples on which methane reaction order is 0.77 on 3-Al-8 and 0.61 on 3-Al-11, further confirming the change in chemical nature of the latter sample due to high temperature treatment that brings an irreversible deactivation.

Saracco et al. [15] found first-order dependence on CH_4 concentration of methane oxidation rate over MgO supported $LaCr_xMg_{1-x}O_3$ catalysts and a general weak effect of oxygen concentration on the reaction kinetics. In particular, a zero order for O_2 was reported on the unsubstituted $LaCrO_3$ perovskite, supported or not, thus evidencing a significant difference in methane oxidation kinetics with respect to our 2-Mg-8 and 2-Mg-11 samples. Future work should be devoted to further investigate the mechanism producing an apparent CH_4 reaction order lower than 1 for

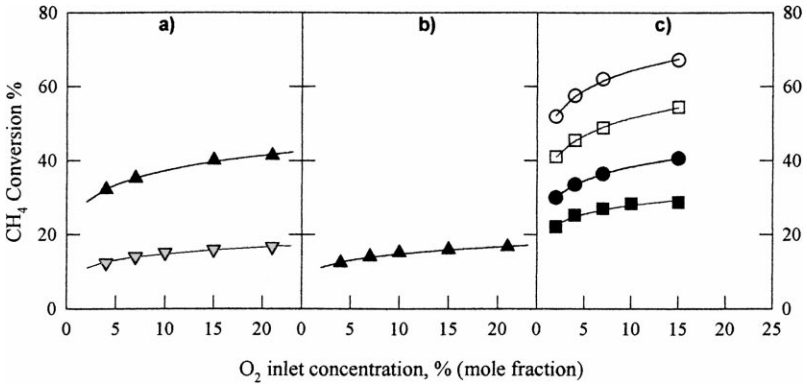

Fig. 5. Methane conversion as a function of the O_2 inlet concentration over 3-Al-8 (a), 2-Mg-8 (b) and 2-Mg-11 (d). Temperature=450 (▽), 500 (▲), 550 (■), 575 (●), 600 (□), 620°C (○). W/F=0.09 g·s/N cm^3. CH_4 inlet concentration 0.4 vol.%.

$LaMnO_3$ and its reduction after dispersion on high surface area supports.

3.4. Monolithic reactor

The catalytic properties of the monolithic system have been evaluated by carrying out activity tests for methane combustion in the same experimental conditions investigated on powders. Fig. 6(a) reports the conversion plots for the monolith as compared with the 3-Al-8 sample with the same chemical composition. Conversions over monolith catalyst are always higher than the corresponding ones over 3-Al-8 powders, either comparing them at the same value of space velocity (flow rate/reactor volume) or areal velocity (flow rate/catalyst wetted surface).

Moreover, Table 4 reports the value of T_{10}, T_{50} and T_{90} measured with the same space velocity used by Zwinkels et al. [12] (46 000 h^{-1}). It appears that our monolithic catalyst exhibit an higher activity, probably

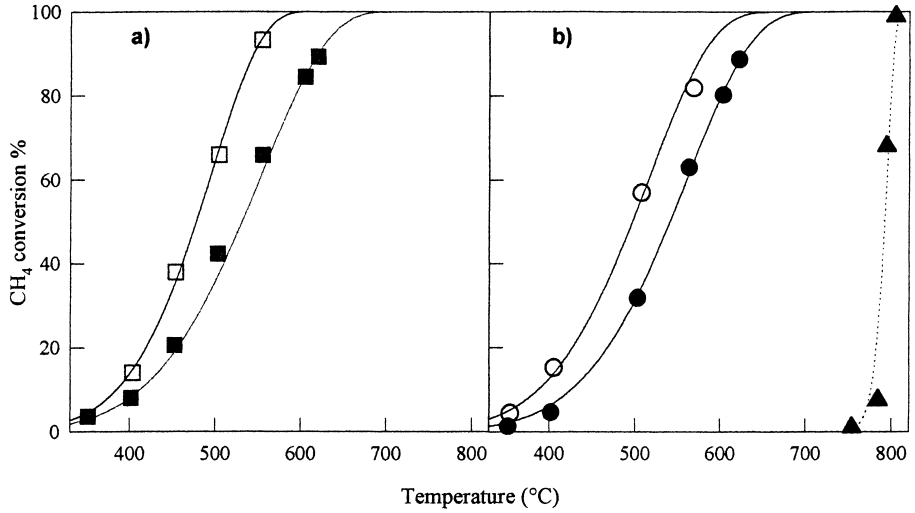

Fig. 6. Effect of temperature on methane combustion for monolith catalysts (0.4% CH_4, 10% O_2). (a) Comparison of monolith (□) and 3-Al-8 sample (■) at the same areal velocity; (b) comparison of fresh (○) and aged (●, 2 h under reaction at 1050°C) monolith with a cordierite sample (▲) (W/F=0.055 g·s/N cm^3). Continuous lines represent fittings with parameters obtained from kinetic analysis.

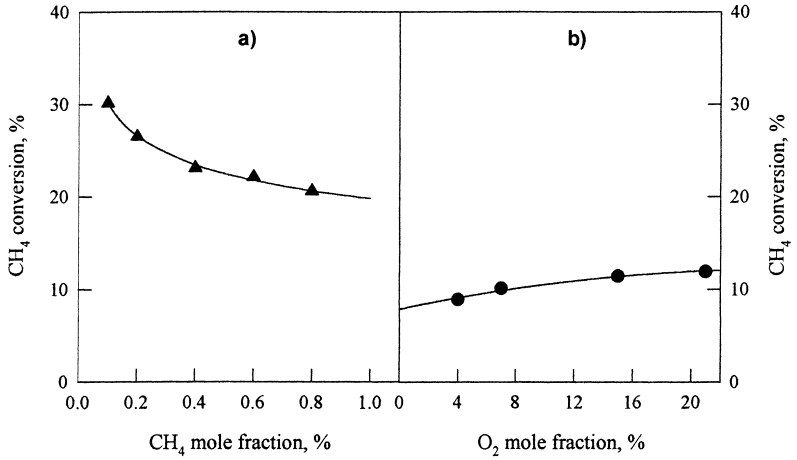

Fig. 7. Methane conversion as a function of the inlet CH_4 (a) and O_2 (b) concentration on monolith catalyst. T=500 (▲) and 420°C (●). W/F=0.09 g·s/N cm^3. O_2 inlet concentration 10 vol.% in (a); CH_4 inlet concentration 0.4 vol.% in (b).

related to the better performances in methane combustion of $LaMnO_3$ catalyst with respect to $LaCrO_3$ [8,9].

Fig. 6(b) reports the conversion plot for fresh monolithic catalyst compared with that of the same sample aged under reaction at 1050°C for 2 h, showing a surprising lower deactivation due to thermal treatment at elevated temperature with respect to the corresponding powder catalyst. Further investigation is needed on this phenomenon and will be required to future work. At the moment, a possible interpretation could be related to a better dispersion of active phase on support due to repeated cycles of deposition necessary to obtain the target loading. Fig. 6(b) also shows conversion data measured on a nude cordierite monolith, revealing no activity of cordierite in methane combustion, since CH_4 is converted to CO and CO_2 only at temperatures at which the homogeneous reactions take place.

The Arrhenius plot obtained from the activity data gives the same value of activation energy of the corresponding powder catalysts 3-Al-8 (18.2 kcal/mol). This result suggests that the chemical nature of the active sites on monolithic and powder catalyst is unchanged. The activation energy obtained by Ciambelli et al. [14] on extruded $La_xCe_{1-x}MnO_3$ monolithic reactor is slightly higher (21.5 kcal/mol), although a not complete selectivity to CO_2 was found. After ageing at 1050°C the calculated activation energy for the monolith sample increases to 19.1 kcal/mol, a value much lower than that estimated for 3-Al-11, as a further confirmation of the reduced deactivation.

The reaction kinetics exhibits a behaviour similar to that shown by 3-Al-8 powders. Fig. 7 shows that methane conversion is a decreasing function of CH_4 inlet concentration while it increases with increasing O_2 concentration, with estimated reaction orders very similar to those found for the supported powder catalyst, as reported in Table 5.

4. Conclusions

$LaMnO_3$ perovskites supported on both lanthanum stabilised γ-Al_2O_3 and MgO have shown high activity in methane combustion. The investigation on La/γ-Al_2O_3 supported samples revealed a dramatic deactivation of the catalyst powders after ageing at 1100°C, due to a strong interaction between the active phase and the support.

On the other hand, cordierite monoliths coated with the same $LaMnO_3$ supported on La/γ-Al_2O_3 show higher activity and thermal stability than the corresponding powder catalyst.

Promising results have also been obtained on MgO supported $LaMnO_3$ samples, whose high activity is associated with remarkable thermal stability. Further investigation is needed in order to set up novel prepa-

ration methods to coat monoliths with MgO supported perovskites.

Acknowledgements

We acknowledge the precious advices of Prof. Paolo Ciambelli (University of Salerno, Italy) on the final drafting of the paper. Special thanks go to Chris Flatley (University of Bath) who spent a 3-month Socrates period in our Institute and contributed for a large part of the experimental campaign.

References

[1] M.F.M. Zwinkels, S.G. Jaras, P.G. Menon, in: A. Cybulski, J. Moulijn (Eds.), Structured Catalysts and Reactors, Marcel Dekker, New York, 1998, p. 149.
[2] Z.R. Ismagilov, M.A. Kerzhentsev, Catal. Rev. Sci. Eng. 32 (1990) 51.
[3] R. Dalla Betta, Catal. Today 35 (1997) 129.
[4] M.F.M. Zwinkels, S.G. Jaras, P.G. Menon, T.A. Griffin, Catal. Rev. Sci. Eng. 26 (1993) 319.
[5] R.A. Dalla Betta, J.C. Schlatter, D.K. Yee, D.G. Loffler, T. Soji, Catal. Today 26 (1995) 329.
[6] K. Eguchi, H. Arai, Catal. Today 29 (1996) 379.
[7] L.G. Tejuca, J.L.G. Fierro, J.M.D. Tascon, Adv. Catal. 36 (1989) 237.
[8] H. Arai, T. Yamada, K. Eguchi, T. Seyama, Appl. Catal. 26 (1986) 265.
[9] J.G. McCarty, H. Wise, Catal. Today 8 (1990) 231.
[10] H.M. Zhang, Y. Teraoka, N. Yamazoe, Appl. Catal. 41 (1988) 137.
[11] B. De Collongue, E. Garbowski, M. Primet, J. Chem. Soc., Faraday Trans. 87 (1991) 2493.
[12] M.F.M. Zwinkels, O. Haussener, P.G. Menon, S.G. Jaras, Catal. Today 47 (1999) 115.
[13] P.E. Marti, M. Maciejewski, A. Baiker, Appl. Catal. B 4 (1994) 225.
[14] P. Ciambelli, V. Palma, S.F. Tikhov, V.A. Sadykov, L.A. Isupova, L. Lisi, Catal. Today 47 (1999) 199.
[15] G. Saracco, G. Scibilia, A. Iannibello, G. Baldi, Appl. Catal. B 8 (1996) 229.
[16] S. Arnone, G. Busca, L. Lisi, F. Milella, G. Russo, M. Turco, Proceedings of the 27th Symposium on Combustion, The Combustion Institute, Boulder, 1998.
[17] J.S. Church, N.W. Cant, D.L. Trimm, Appl. Catal. A 101 (1993) 105.
[18] H. Arai, M. Machida, Appl. Catal. A 138 (1996) 161.
[19] I. Matsuura, Y. Hashimoto, E. Takahaysu, K. Nitta, Y. Yoshida, Appl. Catal. 74 (1991) 273.
[20] M. Berg, S.G. Jaras, Appl. Catal. A 114 (1994) 227.
[21] M. Berg, S.G. Jaras, Catal. Today 26 (1995) 223.
[22] S. Irandoust, B. Andersson, Catal. Rev. Sci. Eng. 30 (1988) 341.
[23] A. Cybulski, J.A. Moulijn, Catal. Rev. Sci. Eng. 36 (1994) 179.
[24] S.T. Kolaczkowski, Trans. Instn. Chem. Engrs 73 (1995) 168.
[25] J.W. Geus, J.C. van Giezen, Catal. Today 47 (1999) 169.
[26] X. Xu, J.A. Moulijn, in: A. Cybulski, J. Moulijn (Eds.), Structured Catalysts and Reactors, Marcel Dekker, New York, 1998, p. 599.
[27] M. Skoglundh, H. Johansson, L. Lowendhal, K. Jansson, L. Dhal, B. Hirschauer, Appl. Catal. B 7 (1996) 299.
[28] L. Lisi, G. Bagnasco, P. Ciambelli, S. De Rossi, P. Porta, G. Russo, M. Turco, J. Solid State Chem. 146 (1999) 176.